MINISTRY OF EDUCATION AND TRAINING
VIETNAM ACADEMY OF SCIENCE AND TECHNOLOGY
GRADUATE UNIVERSITY OF SCIENCE AND TECHNOLOGY

o0o

Tran Van Ngoc

TESTING CP AND CPT INVARIANCES WITH NEUTRINO OSCILLATION MEASUREMENTS IN T2K EXPERIMENT

Summary of Doctoral Thesis in Physics

Major: Mathematical Physics and Theoretical Physics

Code: 9440103

Hanoi, 2023

This thesis was completed at Graduate University of Science and Technology, Vietnam Academy of Science and Technology

Supervisor 1: Assoc. Prof. Nguyen Thi Hong Van, Institute of Physics, Vietnam Academy of Science and Technology
Supervisor 2: Prof. Tsuyoshi Nakaya, Kyoto University, Japan

Referee 1: Prof. Nguyen Van Do, Duy Tan University
Referee 2: Dr. Le Duc Ninh, Phenikaa University
Referee 3: Assoc. Prof. Phan Hong Lien, Military Technical Academy

The thesis was defended at Graduate University of Science and Technology - Vietnam Academy of Science and Technology at 9h00, July 20th, 2023

The thesis can be found at:
- Library of Graduate University of Science and Technology
- National Library of Vietnam

Introduction

Discrete symmetries, including charge conjugation C, parity inversion P, and time reversal T play a vital role in particle physics. Their conservation or violation, individual or in combination, may be the key to unveil the secrets of the universe. Motivating experiments to test CP and CPT invariances is interesting and important in both theoretical and experimental aspects. If CP symmetry is violated in the lepton sector, it may be able to explain the matter - antimatter asymmetry of the univerrse. If CPT is proved to be not conserved, the impact on fundamental physics is enormous. CPT violation can also be a candidate to explain matter-antimatter asymmetry of the universe.

The purpose of this thesis is to investigate the current status and future prospects of testing the CP and CPT invariances from the analysis of recent T2K data and the sensitivity of the synergy of T2K-II, NOνA extension (denoted by NOνA-II from now on), and JUNO experiments. In addition to the introduction and conclusion sections, the thesis consists of three chapters. In Chapter 1, we introduce a general overview of neutrino oscillation phenomenon and relevant experiments. Chapter 2 presents basic results on neutrino flux and beam profile at T2K near detector INGRID which we had directly done the measurement and simulation during the time at J-PARC in 2019. The subject of Chapter 3 is about CP and CPT testing in the T2K experiment and with the joint fit of the T2K-II, NOvA-II, and JUNO experiments.

Chapter 1. Neutrino oscillation phenomenon and experiments

1.1 Neutrino oscillation

Neutrino oscillation is a quantum mechanical phenomenon in which one type of neutrino "oscillates" or transforms into another type during propagation.

1.1.1 Neutrino history

In 1930, W. Pauli suggested the existence of *neutrino* to explain the continuous spectrum behavior in beta decay. The electron neutrino was discovered by Clyde Cowan, Frederick Reines and their colleagues. In 1962, Leon M. Lederman, Melvin Schwartz and Jack Steinberger discovered muon neutrino. Tau neutrino was found in July 2000 by the DONUT collaboration.

1.1.2 Neutrino in Standard Model

In the SM, neutrinos are left-handed and antineutrinos are right-handed particles. They are massless and only participate in the weak interaction.

1.1.3 Neutrino mass and seesaw mechanism

The seesaw mechanism allows to generate mass terms for neutrinos which have one light neutrino state $|m_\nu| \approx \frac{m_D^2}{M}$ and one heavy neutrino state $m_N \approx M$.

1.1.4 Neutrino oscillation in vacuum

The flavor eigenstates are related to the mass eigenstates by a

3×3 uniraty mixing matrix, so-called PMNS matrix.

$$|\nu_\alpha\rangle = \sum_{i=1}^{3} U^*_{\alpha i}|\nu_i\rangle, \tag{1.1}$$

The oscillation probability is defined as

$$\begin{aligned} P(\nu_\alpha \to \nu_\beta) = \delta_{\alpha\beta} \quad &- \quad 4\sum_{i>j} Re\left[U^*_{\alpha i}U_{\beta i}U_{\alpha j}U^*_{\beta j}\right]\sin^2\left(\frac{\Delta m^2_{ij}}{4E}L\right) \\ &+ \quad 2\sum_{i>j} Im\left[U^*_{\alpha i}U_{\beta i}U_{\alpha j}U^*_{\beta j}\right]\sin\left(\frac{\Delta m^2_{ij}}{2E}L\right) \end{aligned} \tag{1.2}$$

where $\Delta m^2_{ij} = m^2_i - m^2_j$. The formula for antineutrino can be achieved by taking the complex conjugate of the product matrix. The *survival probabilities* for a flavor α is

$$P(\nu_\alpha \to \nu_\alpha) = P(\bar{\nu}_\alpha \to \bar{\nu}_\alpha) = 1 - 4\sum_{i>j}|U_{\alpha i}|^2|U_{\alpha j}|^2\sin^2\left(\frac{\Delta m^2_{ij}}{4E}L\right). \tag{1.3}$$

1.1.5 Neutrino oscillation in matter

We can derive the general form of oscillation probability of neutrino in matter as follows

$$\begin{aligned} P(\nu_\alpha \to \nu_\beta) \quad \approx \quad & \delta_{\alpha\beta}\left\{1 - 4|U_{\alpha 3}|^2\sin^2\Delta_{31}\left[1 - \frac{2a}{\Delta m^2_{31}}\left(|U_{13}|^2 - \delta_{\alpha 1}\right)\right]\right. \\ & \left. - \frac{ax}{E}|U_{\alpha 3}|^2|U_{13}|^2\sin 2\Delta_{31}\right\} \\ & + 4\sin^2\Delta_{31}|U_{\beta 3}|^2|U_{\alpha 3}|^2\left[1 - 2\frac{a}{\Delta m^2_{31}}(2|U_{13}|^2 - \delta_{\alpha 1} - \delta_{\beta 1})\right] \\ & - 8\Delta_{21}\sin^2\Delta_{31}Im(U^*_{\beta 3}U_{\alpha 3}U_{\beta 2}U^*_{\alpha 2}) \\ & + 4\Delta_{21}\sin 2\Delta_{31}Re(U^*_{\beta 3}U_{\alpha 3}U_{\beta 2}U^*_{\alpha 2}) \\ & + \frac{ax}{E}\sin 2\Delta_{31}\left(|U_{13}|^2\delta_{\alpha 1}\delta_{\beta 1} + |U_{\beta 3}|^2|U_{\alpha 3}|^2(2|U_{13}|^2 - \delta_{\alpha 1} - \delta_{\beta 1})\right). \end{aligned} \tag{1.4}$$

For anti-neutrino, $P(\overline{\nu}_\alpha \to \overline{\nu}_\beta)$ can be obtained from Eq.(1.4) by taking the complex conjugation of the matrix element product and converting $a \to -a$. The terms containing factor a are related to the matter effect.

1.2 Introduction to some neutrino oscillation experiments

1.2.1 The T2K experiment

T2K is an off-axis accelerator-based long baseline neutrino oscillation experiment located in Japan. It uses muon neutrino and muon antineutrino beams produced at the J-PARC to study oscillations. T2K has three near detectors including the on-axis INGRID, the off-axis ND280, and the WAGASCI-BabyMIND. The T2K far detector, Super-K, is a 50 kiloton water Cherenkov detector located 295km from the neutrino target. It can detect neutrino signal by observing associated lepton particle which emits the Cherenkov light in the detector environment. Super-K is able to discriminate between electron neutrino and muon neutrino very well. T2K-II is a proposal to extend the T2K run until 2027 with total exposure of 20×10^{21} POT, allowing T2K to explore CP violation with a confidence level of 3σ or higher if δ_{CP} is close to $-\pi/2$.

1.2.2 The NOvA experiment

Ongoing NOνA is also an accelerator-based long baseline neutrino experiment which is located in the US. It adopts similar operating principle and off-axis technique as the T2K. NOνA plans to extend it run through 2024 which we call NOνA extension or NOνA-II.

1.2.3 The JUNO experiment

Jiangmen Underground Neutrino Observatory (JUNO) is a reactor-based medium-baseline neutrino experiment located in China. JUNO studies the oscillation of electron antineutrino which flux is produced by the nuclear reactions at the nuclear power plants.

Chapter 2. Measurements at INGRID - the T2K on-axis near detector

2.1 Neutrino flux prediction

For the present operation at 250 kA and future setup at 320 kA horn configurations, the signal neutrino fluxes increase about 13-14 times and 14-15 times at neutrino peak energy (about 1GeV at INGRID location) compared to without horn current applied, respectively.

2.2 Event rate measurement

2.2.1 Simulation of neutrino interactions with NEUT

NEUT is a Monte Carlo simulation package studying interaction of neutrino with nucleus and nucleon from tens of MeV to hundreds of TeV energy range.

2.2.2 Event selection

We follow the event selection procedure for INGRID. The selection follows eight steps including:

1. Time clustering.
2. Number of continuous active planes selection.
3. Two-dimensional track reconstruction.
4. Three-dimensional track reconstruction.
5. Vertexing.
6. Beam timing cut.
7. Upstream VETO cut.
8. Fiducial volume cut.

	Data [/10^{14} POT]	MC [/10^{14} POT]	Data/MC [/10^{14} POT]
run1	1.710 ± 0.002(stat.) ± 0.015(sys.)	1.748	0.978 ± 0.001(stat.) ± 0.009(sys.)
run2	1.746 ± 0.001(stat.) ± 0.016(sys.)	1.748	0.999 ± 0.001(stat.) ± 0.009(sys.)
run3c	1.739 ± 0.001(stat.) ± 0.016(sys.)	1.748	0.995 ± 0.001(stat.) ± 0.009(sys.)
run8a	1.700 ± 0.001(stat.) ± 0.015(sys.)	1.748	0.973 ± 0.001(stat.) ± 0.009(sys.)
run8b	1.702 ± 0.001(stat.) ± 0.015(sys.)	1.748	0.974 ± 0.001(stat.) ± 0.009(sys.)
run8c	1.699 ± 0.001(stat.) ± 0.015(sys.)	1.748	0.972 ± 0.001(stat.) ± 0.009(sys.)
run9	1.697 ± 0.001(stat.) ± 0.015(sys.)	1.748	0.971 ± 0.001(stat.) ± 0.009(sys.)
run10	1.694 ± 0.001(stat.) ± 0.015(sys.)	1.748	0.969 ± 0.001(stat.) ± 0.009(sys.)

Table 2.1: Event rate comparison between FHC runs and MC with +250kA horn operation.

	Data [/10^{14} POT]	MC [/10^{14} POT]	Data/MC [/10^{14} POT]
run5	0.560 ± 0.0010(stat.) ± 0.0094(sys.)	0.565	0.991 ± 0.001(stat.) ± 0.017(sys.)
run6	0.554 ± 0.0004(stat.) ± 0.0093(sys.)	0.565	0.981 ± 0.001(stat.) ± 0.017(sys.)
run7	0.555 ± 0.0004(stat.) ± 0.0093(sys.)	0.565	0.982 ± 0.001(stat.) ± 0.017(sys.)

Table 2.2: Event rate comparison between RHC runs and MC with -250kA horn operation.

2.2.3 Systematic uncertainties

The systematic error of Data/MC is the INGRID detector systematic error of the total number of events selected in all modules, not including uncertainties of flux and neutrino interaction. The total systematic error is calculated to be 0.91% for the neutrino mode and 1.67% for the anti-neutrino mode.

2.2.4 The event rate at INGRID

Tables 2.1 and 2.2 summarize the comparison between our MC simulation and data at INGRID.

	Horizontal center [cm]	Vertical center [cm]
FHC 250kA	2.33 ± 0.89	-0.24 ± 0.99
FHC 320kA	2.53 ± 0.67	-1.27 ± 0.72
RHC 250kA	2.93 ± 0.96	-0.56 ± 1.65
RHC 320kA	1.94 ± 1.11	-0.49 ± 1.19

Table 2.3: Summary of INGRID MC beam center with 250 kA and 320 kA horn operations.

2.3 Beam profile measurement

For T2K run 10, the measurements of neutrino beam direction are stable with a requirement within 1 mrad:

$$\bar{\theta}_H = -0.055 \pm 0.013(\text{stat.}) \pm 0.096(\text{sys.}) \text{ mrad}, \quad (2.1)$$

$$\bar{\theta}_V = 0.085 \pm 0.014(\text{stat.}) \pm 0.106(\text{sys.}) \text{ mrad}. \quad (2.2)$$

The data to MC ratio of beam width is calculated for 250 kA horn operation as follow:

$$W(\text{Data/MC})_H = 1.016 \pm 0.004(\text{stat.}), \quad (2.3)$$

$$W(\text{Data/MC})_V = 1.009 \pm 0.004(\text{stat.}). \quad (2.4)$$

The particular values of the beam center of the horizontal module and vertical module for both FHC mode and RHC mode are summarized in Table 2.3 for 250 kA and 320 kA horn operations. The bias of expected beam directions corresponding to the centers is calculated as shown in Table 2.5.

The measurement of neutrino event rate, beam direction and beam width are in good agreement with MC study.

	Horizontal width [cm]	Vertical width [cm]
FHC 250kA	430.162 ± 1.429	454.508 ± 1.682
FHC 320kA	388.378 ± 0.962	399.982 ± 1.088
RHC 250kA	451.607 ± 2.444	483.255 ± 3.033
RHC 320kA	408.151 ± 1.680	423.141 ± 1.906

Table 2.4: Summary of INGRID MC beam width with 250 kA and 320 kA horn operations.

	Horizontal center [mrad]	Vertical center [mrad]
FHC 250kA	0.084 ± 0.032	-0.009 ± 0.036
FHC 320kA	0.091 ± 0.024	-0.046 ± 0.026
RHC 250kA	0.106 ± 0.035	-0.020 ± 0.060
RHC 320kA	0.070 ± 0.040	-0.018 ± 0.044

Table 2.5: Summary of INGRID beam direction MC with 250 kA and 320 kA horn operations.

2.4 Conclusion

The comparison shows good agreement between the MC results and the T2K data up to runs 10 for 250 kA horn operation. At 320 kA operation, the expected event rates are 2.209 [/10^{14} POT] and 0.664 [/10^{14} POT] for neutrino mode and anti-neutrino mode, respectively. The expected beam directions with respect to the centers of the neutrino mode are 0.091 $\pm$ 0.024 mrad for horizontal and -0.046 $\pm$ 0.026 mrad for vertical. For anti-neutrino mode, the corresponding values are 0.070 $\pm$ 0.040 mrad and -0.018 $\pm$ 0.044 mrad.

Chapter 3. Testing CP and CPT invariances with neutrino oscillation measurements in T2K experiment

3.1 C, P, and T symmetries

3.1.1 Charge conjugation C

Charge conjugation transforms a particle into its antiparticle and vice versa.

$$C|p\rangle = |\overline{p}\rangle, \tag{3.1}$$

where $|p\rangle$ and $|\overline{p}\rangle$ represent particle and antiparticle states, respectively.

3.1.2 Parity inversion P

The parity transformation is associated to spatial inversion through the origin

$$(t, x, y, z) \rightarrow (t, -x, -y, -z). \tag{3.2}$$

3.1.3 Time reversal T

Time reversal is a transformation that takes the sign of time to be opposite

$$(t, x, y, z) \rightarrow (-t, x, y, z). \tag{3.3}$$

3.2 Testing CP invariance with neutrino oscillation experiments

3.2.1 Testing CP invariance in neutrino oscillation

The difference between the neutrino and antineutrino oscillation

probabilities indicates CP violation

$$\begin{aligned}\mathcal{A}_{\rm CP} &= P(\nu_\mu \to \nu_e) - P(\bar{\nu}_\mu \to \bar{\nu}_e) \\ &= 16 c_{12} s_{12} c_{13}^2 s_{13} c_{23} s_{23} \sin\delta_{CP} \sin\frac{\Delta m_{21}^2 L}{4E} \sin\frac{\Delta m_{31}^2 L}{4E} \sin\frac{\Delta m_{32}^2 L}{4E}.\end{aligned} \tag{3.4}$$

In equation (3.4), a quantity for evaluating CP violation that is independent of parameterization, Jarlskog invariant J, is defined as

$$\begin{aligned} J &= \sum_{i>j} Im\left[U_{\alpha i}^* U_{\beta i} U_{\alpha j} U_{\beta j}^*\right] \\ &= c_{12} s_{12} c_{13}^2 s_{13} c_{23} s_{23} \sin\delta_{CP}. \end{aligned} \tag{3.5}$$

In quark sector, Jarlskog invariant is measured precisely

$$J_{quark} = 3.18 \pm 0.15 \times 10^{-5}. \tag{3.6}$$

In the lepton sector, Jarlskog invariant is

$$J_{lepton} \approx -2.25 \times 10^{-2}. \tag{3.7}$$

From Figure 3.1, we can see that CP violation in the quark sector is too small to explain the matter-antimatter asymmetry of the universe, while CP violation in lepton (if confirmed, at least with current values of oscillation parameters) could well do so.

3.2.2 Testing CP invariance with T2K experiment

In 2021, the T2K experiment reported the updated analysis of 3.13×10^{21} POT. Figure 3.2 shows the distribution of $\Delta\chi^2$ function versus δ_{CP}, with and without constraint from reactor, for both neutrino mass ordering cases. The best-fit values and 1σ confidence intervals for δ_{CP} in both mass ordering scenarios are summarized in Table 3.1, with and without constraint from $\sin^2\theta_{13}$ from reactors.

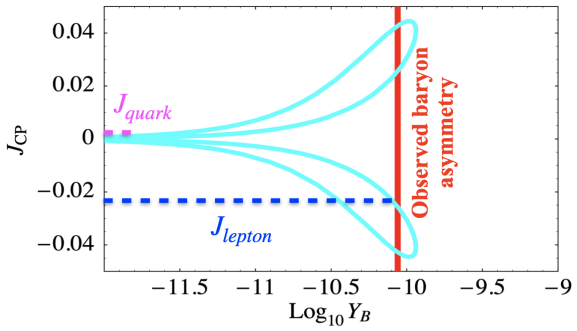

Figure 3.1: The Jarlskog invariant versus the baryon asymmetry varying $\delta_{CP} = [0, 2\pi]$ (cyan). The red region denotes the 2σ range for the baryon asymmetry. The blue line denotes value of Jarlskog invariant in the lepton sector.

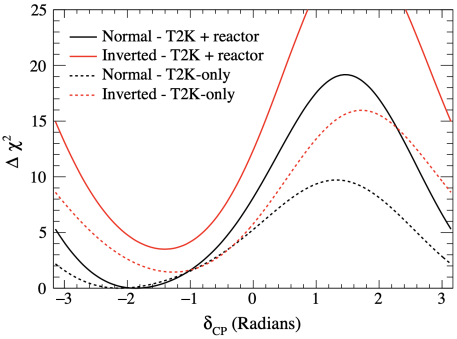

Figure 3.2: The $\Delta\chi^2$ distribution as a function of δ_{CP}, with and without reactor constraint.

Parameters	NO	IO
δ_{CP} (T2K only)	$-2.14^{+0.90}_{-0.69}$	$-1.26^{+0.61}_{-0.69}$
δ_{CP} (T2K+reactor)	$-1.89^{+0.70}_{-0.58}$	$-1.38^{+0.48}_{-0.55}$

Table 3.1: The best fit and best fit $\pm 1\sigma$ intervals of δ_{CP} for T2K only and T2K+reactor for normal and inverted hierarchies. The $\pm 1\sigma$ interval corresponds to the values for which $\Delta\chi^2 \leq 1$.

3.2.3 Testing CP invariance with joint fit of T2K-II, NOνA-II, and JUNO

GLoBES setup for simulating T2K-II, NOvA-II, and JUNO experiments

We provide GLoBES the setups of the three experiments including neutrino flux, cross section, detector mass, detection efficiency. The oscillation probability, event rate, and χ^2 value can be exported.

CP violation sensitivity

Fig. 3.3 shows the CPV sensitivity as a function of the *true* value of δ_{CP} for both MH options. At δ_{CP} close to $-\pi/2$, the sensitivity of the joint analysis with all considered experiments can reach approximately the 5σ C.L. We also calculate the statistical significance of the CPV sensitivity as a function of *true* δ_{CP} at different values of θ_{23}, as shown in Fig. 3.4. Table 3.2 shows the fractional region of all possible *true* $\delta_{\rm CP}$ values for which we can exclude CP conserving values of $\delta_{\rm CP}$ to at least the 3σ C.L., obtained by the joint analysis of all considered experiments.

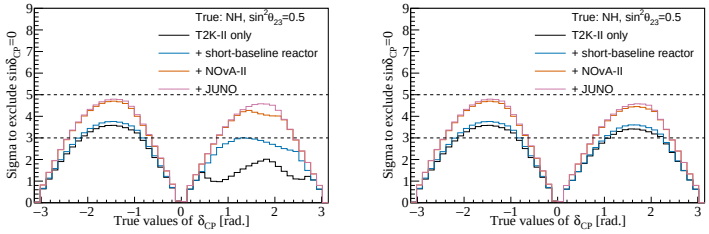

Figure 3.3: CPV sensitivity as a function of the *true* value of δ_{CP} obtained with different analyses. *Normal* MH and $\sin^2\theta_{23} = 0.5$ are assumed to be *true*. Left (right) plot is with the MH assumed to be *unknown* (*known*) in the analysis respectively.

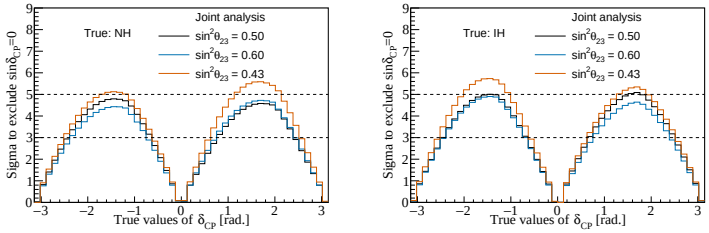

Figure 3.4: CPV sensitivity as a function of the *true* value of δ_{CP}. Left (right) plot is with the *normal* (*inverted*) MH respectively assumed to be true. MH is assumed to be *unknown* in the analysis.

Value of $\sin^2\theta_{23}$	0.43	0.50	0.60
Fraction of *true* δ_{CP} values (%), NH	61.6	54.6	53.3
Fraction of *true* δ_{CP} values (%), IH	61.7	57.2	54.2

Table 3.2: Fractional region of δ_{CP}, depending on $\sin^2\theta_{23}$, can be explored with 3σ or higher significance.

3.3 Testing CPT invariance with neutrino oscillation experiments

3.3.1 Testing CPT invariance in neutrino oscillation

The CPT theorem states that all interactions described by a unitary, local, Lorentz-invariant quantum field theory in a flat Minkowski space must be invariant under the combined CPT transformation.

Under CPT symmetry, the oscillation probability is transformed as follows:

$$P(\nu_\alpha \to \nu_\beta) \xrightarrow{CPT} P(\overline{\nu}_\beta \to \overline{\nu}_\alpha).$$

If CPT is violated, the asymmetry can be evaluated as

$$\mathcal{A}_{\alpha\beta}^{CPT} = P(\nu_\alpha \to \nu_\beta) - P(\overline{\nu}_\beta \to \overline{\nu}_\alpha). \tag{3.8}$$

T2K and NOνA experiments focus on four channels, including two appearance channels ($\nu_\mu \to \nu_e$, $\overline{\nu}_\mu \to \overline{\nu}_e$), and two disappearance channels ($\nu_\mu \to \nu_\mu$, $\overline{\nu}_\mu \to \overline{\nu}_\mu$). T2K and NO$\nu$A alone can test CPT invariance via their measurements of the disappearance channels which are sensitive to the CPT asymmetric quantities $\mathcal{A}_{\mu\mu}^{CPT}(\sin^2\theta_{23})$ and $\mathcal{A}_{\mu\mu}^{CPT}(\Delta m^2_{31})$.

3.3.2 GLoBES setup for simulating T2K-II, NOvA-II, and JUNO experiments

We basically follow the GLoBES setup for T2K-II, NOνA-II, and JUNO as in the previous section. For T2K-II and NOνA-II, we used the disappearance channels only, with statistics equally divided for ν mode and $\overline{\nu}$ mode. For JUNO, $\overline{\nu}_e$ disappearance data is used. We assume neutrino masses are in normal ordering throughout the study in Sec. 3.3.4.

The sensitivity to rule out CPT invariance hypothesis with $|\delta(X)| = |X - \overline{X}|$ is explored. The χ^2 of individual experiment is calculated for given true values of X and $\overline{X}$, where X can be $\sin^2\theta_{23}$ or Δm^2_{31}. The statistical significance of excluding CPT conservation is expressed as the squared root of the minimum joint $\Delta\chi^2$.

3.3.3 Testing CPT invariance with T2K experiment

The following results are done with GLoBES simulation using 3.13×10^{21} POT. The statistical significance to exclude CPT conservation hypothesis is shown in Figure 3.5 in terms of σ values versus $\delta(\Delta m^2_{31})$ (left) and $\delta(\sin^2\theta_{23})$ (right). The results show no CPT violation signature with the current data of T2K. The expression (3.9) summarizes the CPT violation bounds at 3σ C. L. with $|\delta(\Delta m^2_{31})|$ and $|\delta(\sin^2\theta_{23})|$.

$$\begin{aligned} |\delta(\Delta m^2_{31})| &< 6.35 \times 10^{-4} eV^2, \\ |\delta(\sin^2\theta_{23})| &< 0.19. \end{aligned} \tag{3.9}$$

3.3.4 Testing CPT invariance with joint fit of T2K-II, NOνA-II, and JUNO

Bounds on CPT violation The bounds to CPT violation at 3σ as a function of $|\delta(\Delta m^2_{31})|$ (left) and $\delta(\sin^2\theta_{23})$ (right) are displayed in Fig. 3.6 and summarized in Table 3.3.

Sensitivities to CPT violation The results are shown in Fig. 3.7. If $|\delta(\Delta m^2_{31})| > 5.4 \times 10^{-5} eV^2$, combined analysis of the three experiments is able to exclude CPT conservation at 3σ C. L. If T2K (NOνA) best fits are assumed to be true, the combined analysis of T2K-II, NOνA-II, and JUNO can exclude CPT conservation at 1.7σ (4σ) C. L.

For the mixing angle, the Fig. 3.7 right illustrates the signifi-

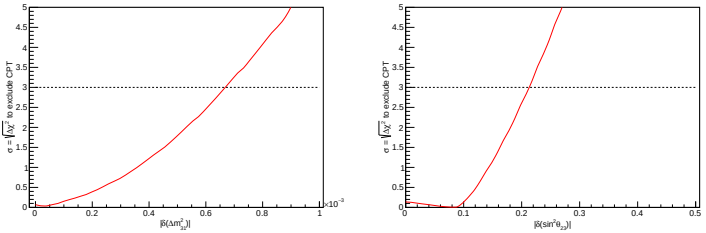

Figure 3.5: Statistical significance to exclude CPT conservation hypothesis with $\delta(\Delta m^2_{31})$ (left) and $\delta(\sin^2\theta_{23})$ (right) for T2K with 3.13×10^{21} POT exposure.

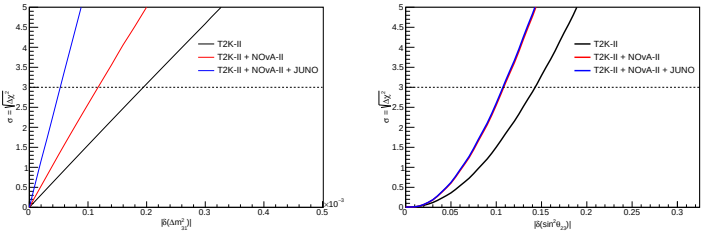

Figure 3.6: The bounds on CPT violation at 3σ C. L. with atmospheric mass squared splittings (left) and mixing angles (right). The black, red, and blue lines are corresponding to T2K-II, T2K-II adding NOνA-II, and T2K-II adding NOνA-II and JUNO, respectively.

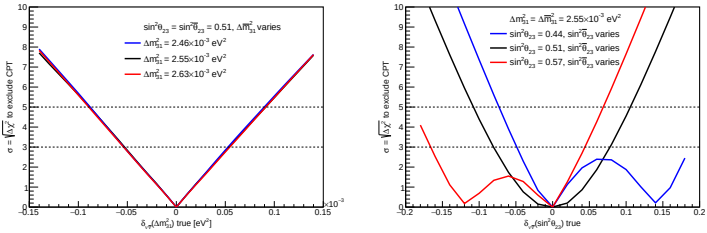

Figure 3.7: The CPT sensitivities are the functions of the true values Δm^2_{31} (left) and $\sin^2\theta_{23}$ (right).

	3σ C. L. upper limits	
Experiments	$\lvert\delta_{\nu\overline{\nu}}(\Delta m^2_{31})\rvert$	$\lvert\delta_{\nu\overline{\nu}}(\sin^2\theta_{23})\rvert$
T2K-II	2.0×10^{-4} eV^2	0.14
T2K-II+NOνA-II	1.2×10^{-4} eV^2	0.10
T2K-II+NOνA-II+JUNO	5.3×10^{-5} eV^2	0.10

Table 3.3: The bounds on CPT violation with atmospheric mass-squared difference and mixing angle at 3σ C. L. for three analyses: T2K-II only, a joint of T2K-II and NOνA-II, a joint of T2K-II, NOνA-II, and JUNO.

	Δm^2_{31}	3σ excluded range of $\lvert\delta(\Delta m^2_{31})\rvert$	3σ excluded range of $\lvert\delta(\sin^2\theta_{23})\rvert$
$2.46\times10^{-3}\ eV^2$	$\geq 5.36\times10^{-5}eV^2$	0.44	≥ 0.187
$2.55\times10^{-3}\ eV^2$	$\geq 5.39\times10^{-5}eV^2$	0.51	≥ 0.080
$2.63\times10^{-3}\ eV^2$	$\geq 5.46\times10^{-5}eV^2$	0.57	≥ 0.166

Table 3.4: The dependence of the CPT sensitivities on the true values.

cant dependence of sensitivity on the true values $\sin^2\theta_{23}$ and $\sin^2\overline{\theta}_{23}$. If the current measurements of T2K (NOνA) is presumed, the combined data can exclude CPT invariance at 3σ (4.6σ) C. L.

Conclusions

Our study in Chapter 2 shows that the event rates, neutrino beam directions, and beam widths are stable and in good agreement between the MC study and the data of T2K run 10. We also showed the MC study at INGRID with a 320 kA horn configuration, which can be tested with future data of T2K.

In Chapter 3, the CP and CPT violation searches with the T2K experiment are presented. The current data of T2K rules out CP conserving hypothesis at more than 90%. With T2K data only, the CP violating phase δ_{CP} is measured to be $-2.14^{+0.90}_{-0.69}$ in case of normal mass ordering and $-1.26^{+0.61}_{-0.69}$ in case of inverted mass ordering. If T2K-II data is combined with NOνA-II and JUNO experiments, CP conservation is excluded at around 5σ C. L.

The study shows there is no signature of CPT violation with current data from T2K. The synergy of T2K-II, NOνA-II, and JUNO will improve the sensitivity and bounds on CPT violation to unprecedented levels of precision. If the recent T2K (NOνA) results on (Δm^2_{31}, $\Delta\overline{m}^2_{31}$) and ($\theta_{23}$, $\overline{\theta}_{23}$) are presumed to be true values, the combined data of the three experiments is able to exclude CPT symmetry at 1.7σ (4σ) and 3σ (4.6σ) C. L., respectively. The synergy of T2K-II, NOνA-II, and JUNO can improve the bound on $|\delta(\Delta m^2_{31})|$ to the world's best value, $5.3 \times 10^{-5} eV^2$ at 3σ C. L. The sensitivity to CPT violation basically does not depend on the true values of Δm^2_{31} and $\Delta\overline{m}^2_{31}$ but on the true values of θ_{23} and $\overline{\theta}_{23}$ as well as their differences.

List of Publications

List of publications used for thesis defense

1. T. V. Ngoc, S. Cao, N. T. Hong Van, and P. T. Quyen. *Stringent constraint on CPT violation with a combined analysis of T2K-II, NOνA extension, and JUNO*. Phys. Rev. D, 107 016013, 2023.

2. S. Cao, A. Nath, T. V. Ngoc, Ng. K. Francis, N. T. Hong Van, and P. T. Quyen. *Physics potential of the combined sensitivity of T2K-II, NOνA extension, and JUNO*. Phys. Rev. D, 103 11 112010, 2021.

List of other publications

1. S. Cao, N. T. Hong Van, T. V. Ngoc, and P. T. Quyen. *Neutrino Mass Spectrum: Present Indication and Future Prospect*. Symmetry, 14 1, 2022.

2. T. V. Ngoc, S. Cao, N. T. Hong Van. *Combined Sensitivity of T2K-II and NOνA Experiments to CP Violation in Lepton Sector*. Commun. in Phys., 28 4, 337, 2018.

3. S. Cao, T. V. Ngoc, N. T. Hong Van, and P. T. Quyen. *Practical use of reactor anti-neutrinos for nuclear safeguard in Vietnam*. Accepted to publish on Commun. in Phys., [arXiv:2209.03541].

4. N. H. Duy Thanh, N. V. Chi Lan, S. Cao, T. V. Ngoc, N. Khoa, N. T. H. Van, and P. T. Quyen. *Multi-pixel photon counter for operating a tabletop cosmic ray detector under loosely controlled conditions*. Dalat University Journal of Science, 13 1, 16-29, 2022.

5. T. V. Ngoc *et. al.* [T2K collaboration]. *T2K measurements of muon neutrino and antineutrino disappearance using* 3.13×10^{21} *protons on target.* Phys. Rev. D, 103 1, L011101, 2021.

6. T. V. Ngoc *et. al.* [T2K collaboration]. *Improved constraints on neutrino mixing from the T2K experiment with* 3.13×10^{21} *protons on target.* Phys. Rev. D, 103 11, 112008, 2021.

7. T. V. Ngoc *et. al.* [T2K collaboration]. *Constraint on the matter–antimatter symmetry-violating phase in neutrino oscillations.* Nature, 580 7803, 339-344, 2020. Nature, 583 7814, E16, 2020 (erratum).